Characterizations of Stiff Chain Macromolecules. Poly(n-hexyl isocyanate) in n-Hexane

Donn N. Rubingh and Hyuk Yu*

Department of Chemistry, University of Wisconsin, Madison, Wisconsin 53706.
Received April 1, 1976

ABSTRACT: The equilibrium characterization of poly(n-hexyl isocyanate) fractions in n-hexane at 25 °C was performed in order to test the two-parameter description of stiff chains vis-a-vis the wormlike-coil model. With use of the scheme proposed by Yamakawa and Fujii for the light scattering and intrinsic viscosity measurements, the ranges of the statistical length and the mass per unit length are determined as 790 Å $\leq \lambda^{-1} \leq$ 850 Å and 78 Å$^{-1} \geq M_L \geq$ 64 Å^{-1}, respectively. Inclusion of the data set obtained by Berger and Tidswell in tetrahydrofuran at 25 °C extends the applicability of these ranges of the parameters without altering them. We did not take into account any excluded volume effect in the analysis because its contribution is suspected to be small except at molecular weights over 10^6. The customary method of independently determining the mass per unit length by applying the rigid rod model to the particle scattering factor at small molecular weight is found to be susceptible to error.

Stiff chain polymers of synthetic or biological origins are characterized by a gradual configurational change, from rodlike to coillike state, as the degree of polymerization is increased. Well studied examples of this change are seen with DNA,[1,2] poly(γ-benzyl L-glutamate),[3,4] cellulose derivatives,[5,6] and poly(n-alkyl isocyanates)[7–9] in terms of their equilibrium chain dimension. Irrespective of a model chosen, the equilibrium linear dimension of stiff chain is characterized by two parameters, i.e., the monomeric projection along the chain contour direction and the persistence length,[9] or their equivalents such as the mass per unit length and the Kuhn statistical length. The equilibrium chain stiffness is then specified by the asymptotic characteristic ratio[10] C_∞ which is directly proportional to the ratio of persistence length to monomeric projection length (see below). Difference among several models lies in the manner of approach to the asymptotic limit with respect to the degree of polymerization.[11] More recently the two-parameter scheme of characterization of stiff chain is called into question in the literature. In particular, apparent dependence of the persistence length on the degree of polymerization has been shown by several groups.[12,13] It appears that inadequacy of the two-parameter characterization is mostly arisen from the dynamic measurements whereas the theory to interpret them[14–16] is far less developed than that for the equilibrium measurements. Meantime there appears to be confusion in the literature with the term "chain stiffness". In the language of the rotational isomeric state theory,[17] it can be clarified as follows: the equilibrium chain stiffness should be determined by the relative energy levels of various rotational isomeric states as appropriately modified by the neighbor correlations while the dynamic chain stiffness ought to be reflected by the barrier heights separating the ground states. The two-parameter description of stiff chain refers to the equilibrium problem.

In this paper, we address the issue of stiff chain characterization in the equilibrium configuration. We will show that two different chain dimensional probes, i.e., light scattering and intrinsic viscosity (at zero shear rate), both give rise to a consistent set of the characteristic parameters, and the two-parameter description is entirely adequate provided that the measurements are performed with a monodisperse series of samples in inert solvents[13,18] at a given temperature.[19]

Experimental Section

Materials. Commercially available n-hexyl isocyanate (Eastman Organic Chemicals) was purified by distillation after drying over a calcium hydride dispersion for 1 week. The polymerizations were carried out in toluene solutions at −78 °C with sodium biphenyl in tetrahydrofuran as the anionic intiator. The "living" polymer was terminated after 1 week and precipitated by the addition of methanol. Upon washing with methanol, the polymer was dried in vacuo (10^{-5} Torr) at room temperature and then further purified by dissolving in toluene and reprecipitating with methanol and drying in vacuo.

The purified samples were dissolved in CCl_4 at low concentration (~2 g/8 l.) for fractionation. The procedure was as follows. Methanol was added to the polymer solution until turbidity developed. The solution was then warmed until the turbidity disappeared (~40 °C) then allowed to cool slowly over a period of 3–4 h to room temperature with the precipitate reforming. The precipitated polymer was collected and dried while the solution was treated similarly to obtain the next fraction. The width at half height of the dielectric loss curve has been shown to be proportional to the sample polydispersity if it is not too large.[20,21] Thus the efficacy of the fractionation procedure could be tested by dielectric measurements. A typical curve is as shown in Figure 1. The sample "polydispersity index" M_w/M_n determined by this method is collected in Table I. The solvent used was n-hexane which was obtained from commercial Skelly B by fractional distillation until the refractive index (n_D) reached 1.3740 ± 0.0005 at 25 °C.

Light Scattering. A SOFICA light scattering photometer was used for all measurements and scattered intensities for angles from 30 to 150° were recorded on a strip chart. The temperature of the sample was maintained at 25.0 ± 0.5 °C and the wavelength of the incident radiation was 5460 Å.

The instrument was calibrated in the following manner. (1) Optical alignment; the distribution of the scattered intensity from benzene was analyzed according to the equation

$$\frac{I(\theta)\sin\theta}{I(90°)} = \frac{1-\rho_\mu}{1+\rho_\mu}(1+\cos^2\theta) \quad (1)$$

where the scattered intensity at a given scattering θ is denoted by $I(\theta)$. The depolarization ratio ρ_μ determined in this manner was 0.40 as compared to the literature value of 0.41.[22] (2) Volume correction; the sin θ dependence of the scattering volume was also observed directly by scattering with dilute fluorescein solutions in ethanol. (3) Molecular weight; the molecular weight of NBS 705 standard polystyrene sample was determined and agreed with the certified molecular weight, 179 000, to within 5%.

The elimination of dust from the polymer solution is a primary concern in obtaining accurate light scattering data. A simple and reliable procedure for clarification of PHIC in hexane was to centrifuge for 1–2 h at 7000 G in centrifuge tubes containing approximately ¾ in. of glass beads at the bottom; the glass beads apparently served to trap the dust and prevented convection current from stirring up the dust when withdrawing the solution from the tubes.

The quantity (dn/dc), the differential refractive increment, was measured using a Brice-Phoenix differential refractometer. Maintaining the n-hexane solution at 25.00 ± 0.01 °C and using the 5460 Å Hg vapor line the value was determined as 0.123 ± 0.001.

Intrinsic Viscosity Measurements. The intrinsic viscosity measurements were carried out in a Cannon-Ubbelohde variable shear rate viscometer. The shear rates of the viscometer with n-hexane were respectively 530, 251, 114, and 45 s^{-1} at four different bulb locations. Calibrations of the viscometer with two liquids, n-hexane and $CHCl_3$, showed negligible kinetic energy correction. For the highest molecular weight sample, the shear rate dependence was pronounced and a reliable extrapolation to zero shear rate required going to a lower shear rate. This was accomplished by using a rotating cylinder viscometer[23]

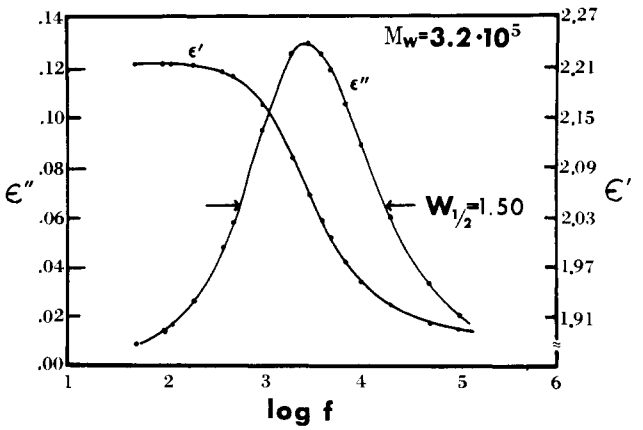

Figure 1. Dielectric dispersion of PHIC in *n*-hexane where the full width at half height of the loss profile is used to deduce M_w/M_n via the correlation provided in ref 20 and 21.

of the Zimm–Crothers[24] type. All measurements were made at 25.00 ± 0.03 °C.

Analysis Methods

Before proceeding with the experimental results, we outline first the methods adopted for the analyses of the two types of measurements.

Light Scattering. Regardless of specific chain configuration, the reciprocal particle scattering factor should be expressed as

$$P^{-1}(\theta) = 1 + \tfrac{1}{3}\langle S^2\rangle q^2 + \ldots \quad (2)$$

in the limit of low scattering angle, where $\langle S^2\rangle$ is the mean square radius of gyration and q is the magnitude of scattering wave vector defined as $(4\pi/\lambda')\sin(\theta/2)$ in terms of the wavelength of light in the scattering medium λ' and the scattering angle θ. The truncation of the series expansion in q^2 at the second term is permissible only when the linear dimension or the scattering angle is small enough to fulfill the condition that $\langle S^2\rangle q^2 \leq 1$. Otherwise, the determination of $\langle S^2\rangle$ from the limiting slope of the Zimm plot could well introduce systematic error. Although a scheme to extend the linear region of the q^2 dependence by taking the square root of $P^{-1}(\theta)$ has been put forth in the literature,[25] we often have to contend with the situation where this is not adequate with stiff chains. Two possible routes to remove the complication are (1) to measure the scattered intensity at sufficiently low angle that the above condition is fulfilled or (2) to deduce the curvature of $P^{-1}(\theta)$ against q^2 from the theory. Since our light scattering instrument cannot measure below 30° such that we are safely in the region of $\langle S^2\rangle q^2 \leq 1$ with high molecular samples, we resort to the second method of matching the complete angular dependence of $P^{-1}(\theta)$ between the experimental and the parametrized theoretical prediction by Yamakawa and Fujii.[26]

Two points need to be made relative to the Y–F method regarding the extreme limits of contour length. The particle scattering factor given by Yamakawa and Fujii for the wormlike-coil model is indistinguishable from that of the rigid rod model for the reduced contour length L_r less than three where the scaling factor is the Kuhn statistical length $(1/\lambda)$, i.e., less than six persistence lengths. This is not unexpected inasmuch as the wormlike-coil model ought to reduce to that of rigid rod in the limit of short contour length. Thus the differentiation of two competing models at low molecular range where the contour length is comparable to the Kuhn statistical length is not possible on the basis of the particle scattering factor. Furthermore, the determination of the mass per unit length directly from the experimental radius of gyration in the rod limit must be attended by assurance that the contour length of the sample is indeed equal or less than the persistence length. This is illustrated in Figure 2; the reciprocal particle scattering factor is plotted against the square of reduced scattering vector for the wormlike-coil model at different reduced contour lengths (solid curves), and the corresponding value (filled circles) for rigid rod model is plotted against the equivalent scattering vector Q^2, defined as $[(4\pi/\lambda')(L/2)\sin(\theta/2)]^2$, where the rod length L is so chosen as to yield best matching with the wormlike-coil model at each L_r. In Table II, we summarize the comparison of parameters deducible from such a matching. For instance, the particle scattering factor of a wormlike-coil whose contour length is equal to $1/\lambda$, i.e., $L_r = 1$, can be fitted perfectly well to rigid rod model with the rod length which is 85% of the statistical length, $L_{rod} = 0.85/\lambda$. On the basis of goodness of fit one cannot distinguish the two. As a consequence, the mass per unit length calculated as a rigid rod overestimates beyond that of wormlike-coil model by 18% or underestimates the monomeric projection by 15%.

Second, we comment on the other side of the contour length range, namely the long chain limit. The analytical expression for the particle scattering factor, given by Sharp and Bloomfield,[27] is known to apply in the long chain limit because it embodies a first-order stiffness correction to the Debye ex-

Table I
Results of Dielectric, Light Scattering, and Viscosity Studies of PHIC in *n*-Hexane

$M_w \times 10^{-5}$ ± 10%	$W_{1/2}$, Hz[a] (log scale)	M_w/M_n[b]	$\langle S^2\rangle^{1/2} \times 10^{-3}$ Å ± 12%	$[\eta]$, dl/g
0.91	2.55	>1.6		3.60
1.0	1.65	1.1	0.38	4.65
3.2	1.50	1.1	0.92	11.2
4.6	1.50	1.1	0.99	
5.2	1.65	1.1	1.1	15.8
7.0	1.55	1.1	1.2	28.2
23	2.40	>1.6	2.0	95.0
55[c]			3.4	

[a] The full width at half height of the dielectric loss in logarithmic frequency. [b] Estimated with use of the correlation provided in ref 20 and 21. [c] The light-scattering measurement of this sample was performed by J. K. Yamamoto in her senior thesis research at the University of Wisconsin–Madison.

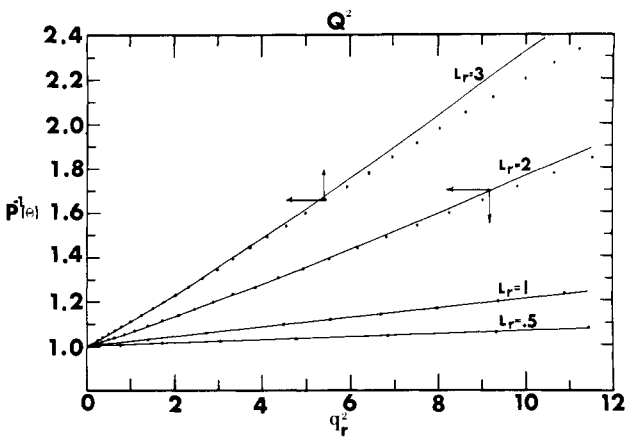

Figure 2. Comparison of two models at short contour lengths. The reciprocal particle scattering factor is plotted against the reduced scattering wave vector for the wormlike-coil model as given by Yamakawa and Fujii (solid curves), and the best matching prediction for the rigid rod model is plotted against Q^2 at each reduced contour length (filled circles); $q_r = (4\pi/\lambda')(1/\lambda)\sin(\theta/2)$ (wormlike-coil) and $Q = (4\pi/\lambda')(L/2)\sin(\theta/2)$ (rigid rod).

Table II
Comparison of the Parameters Calculated from the Wormlike-Coil and the Rigid Rod Models at Small Contour Length from the Particle Scattering Factor Plot in Figure 2

L_r[a]	L(apparent)[b] for rigid rod	M_L(rigid rod)/ M_L(wormlike-coil)	h(rigid rod)[c]/ h(wormlike-coil)
0.5	0.46/λ	1.11	0.90
1	0.85/λ	1.18	0.85
2	1.53/λ	1.31	0.77
3	1.97/λ	1.52	0.66

[a] Reduced contour length of wormlike-coil model. [b] The particle scattering factor plot shown in Figure 2 makes it reasonable to assume that the rigid rod model is applicable, and the apparent length of rod is given here in terms of the corresponding statistical length of the wormlike-coil model. [c] The ratio of monomeric projection lengths calculated on the bases of two models.

pression via the first Daniel's approximation of the segment pair distribution.[28] The expression may be written as

$$P(\theta) = \frac{2}{X^2}(X - 1 + e^{-X}) + \frac{4}{15L_r} + \frac{7}{15XL_r} - \left(\frac{11}{15L_r} + \frac{7}{15XL_r}\right)e^{-X} \quad (3)$$

with $X \equiv q_r^2 L_r/6$, $q_r \equiv (4\pi/\lambda')(1/\lambda)\sin(\theta/2)$, and $L_r \equiv \lambda L$. Here, the first term is the Debye function and the rest represents the stiffness correction. A question is how long a contour length has to be before this sort of correction would suffice? The applicability bound of eq 3 has been operationally defined by Yamakawa and Fujii as $L_r \geq 10$ and $q_r^2 \leq 10$ since they found that eq 3 and their numerical tabulation agreed within 1% for these ranges of L_r and q_r^2. We now show why this is the case.

If $X < 1$ (the longer a contour length becomes, the lower the scattering angles must be to fulfill this condition), eq 3 can be expanded as

$$P(\theta) = 1 - \frac{X}{3} + \frac{q_r^2}{12} - \frac{13}{270}q_r^2 X + O(q_r^2 X^2) = 1 - \frac{q_r^2}{18}\left(L_r - \frac{3}{2} + \frac{13}{15}X - \ldots\right) \quad (4)$$

and

$$P^{-1}(\theta) \approx 1 + \frac{1}{3}\left(\frac{L}{6\lambda} - \frac{1}{4\lambda^2}\right)q^2 - \ldots \quad (5)$$

Equation 5 shows that the mean square radius of gyration is $[(L/6\lambda) - (1/4\lambda^2)]$. On the other hand, the full expression for the mean square radius of gyration of the wormlike-coil[29] is

$$\langle S^2 \rangle = \frac{1}{\lambda^2}\left[\frac{L_r}{6} - \frac{1}{4} + \frac{1}{4L_r} - \frac{1}{8L_r^2}(1 - e^{-2L_r})\right] \quad (6)$$

When L_r is large, eq 6 may be written as

$$\langle S^2 \rangle = \frac{1}{\lambda^2}\left(\frac{L_r}{6} - \frac{1}{4}\right) + O\left(\frac{1}{\lambda^2 L_r}\right) \quad (6')$$

If $L_r = 10$, the approximation afforded by eq 6′ overestimates the exact value by only 1.6%. Hence, eq 5 correctly predicts the mean square radius of gyration of a wormlike-coil within the approximation; the term linear in q^2 of eq 5 is just $[(L/6\lambda) - (1/4\lambda^2)]/3$. The agreement reported by Yamakawa and Fujii therefore should have been expected, and the two conditions, $L_r \geq 10$ and $X < 1$, define the applicability bound of eq 3 in so far as the usual scheme of determining the radius of gyration (in a $P^{-1}(\theta)$ vs. q^2 plot) is concerned.

Parenthetically, we also note that the condition of $X < 1$ for large viral DNA's could place a rather stringent constraint on the experiment. For instance, the $X < 1$ condition for T7 DNA (mol wt 2.5×10^7) requires that the scattering angle be lower than 7° with green light in aqueous media ($\lambda' = 4.1 \times 10^3$ Å) when $\lambda^{-1} = 1.3 \times 10^3$ Å.[1,2] On the other hand, if $P^{-1/2}(\theta)$ is plotted against q^2 the linear region can be extended to 15°, which is within the range of a low-angle instrument reported by Harpst et al.[30] The controversy evoked by Schmid et al.[2] concerning the characterization of DNA seems to be settled by Yamakawa and Fujii.[26]

We would conclude from the foregoing discussion that the determinations of two parameters of the wormlike-coil model are entirely possible according to the Yamakawa–Fujii scheme for the samples having the reduced contour length $L_r \geq 10$ with the aid of $P(\theta)$ expression given by Sharp and Bloomfield. Putting it differently, the available range of molecular weight need not be spanned across the configurational limits, from rod to coil, in order to deduce the wormlike-coil parameters.

Briefly recapitulating the scheme to extract λ^{-1} and M_L from light scattering measurements, we first estimate the ranges of λ^{-1} and M_L by plotting on log–log scale the mean square radius of gyration as obtained from the raw Zimm plot against the molecular weight, and deduce the said range with the aid of eq 6, then plot the observed $P^{-1}(\theta)$ in linear scale against q^2 in logarithmic scale and perform horizontal shifts by $(1/\lambda)^2$ within the estimated range of λ^{-1}. Finally, we match them with the predicted curves at the lower and upper bounds of L_r ($= \lambda M/M_L$) as given by the Y–F tabulation or eq 3, depending on the molecular weight. The best match within the experimental uncertainty of $P^{-1}(\theta)$ provides the final set of λ^{-1} and M_L for a given molecular weight sample. The procedure is repeated with the scattering data of other samples, and the final set of the ranges of λ^{-1} and M_L then reflects the variability among different molecular weight samples.

Intrinsic Viscosity. The Yamakawa–Fujii[31] scheme of determining the wormlike-coil parameters from the relationship of intrinsic viscosity and molecular weight will also be adopted. Unlike the case of light scattering, here the theory calls for a third parameter, the hydrodynamic diameter of wormlike-coil d. The intrinsic viscosity, as given by Yamakawa and Fujii, is expressed as

$$[\eta] = 10^{-2}\Phi(L_r, d_r)M^{1/2}/(\lambda M_L)^{3/2} \quad (7)$$

in dl/g units, where $\Phi(L_r, d_r)$ is provided by Y–F as a function of the reduced quantities of the contour length and diameter where the scaling factor is again λ^{-1}. Thus, the scheme is quite analogous to the estimation of λ^{-1} and M_L from eq 6 in the light scattering case. Because of the additional parameter d required by the theory, proof of uniqueness of the three parameters so determined is not possible. On the other hand, one might attempt to show the reasonableness of d values chosen to represent the data if the same set of λ^{-1} and M_L determined by another measurement, e.g., light scattering, is applicable.

Results and Discussion

The data analysis of light scattering by the Zimm plot was performed on the UNIVAC 1110. A typical Zimm plot is presented in Figure 3. Table I summarizes the results based on the first seven angles (up to 105°). The absolute uncertainty of the molecular weight determination is estimated to be about 10%; the propagation of error starts from 2% due to (dn/dc), 1 and 2% due to the scattered intensity and concentration determinations, respectively, 5–6% arising from extrapolation to zero concentration and angle, and 2% due to the uncertainty of the Rayleigh ratio of benzene which served as

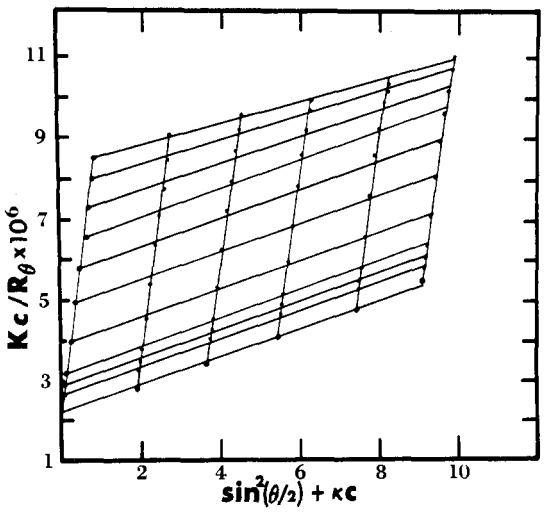

Figure 3. A typical Zimm plot of PHIC in n-hexane (M_w = 4.6 × 10^5).

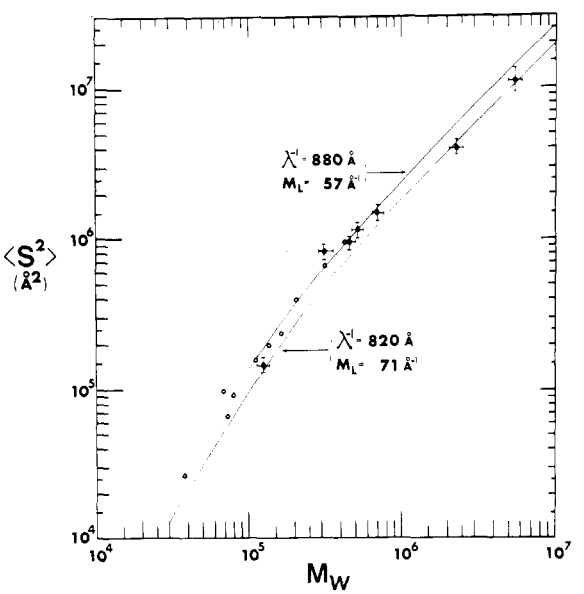

Figure 4. The mean square radius of gyration is plotted against the weight average molecular weight. Filled circles are for PHIC in n-hexane and unfilled circles are for PHIC in tetrahydrofuran from ref 31. Solid curves are drawn according to eq 6 with the ranges of two parameters, 820 Å ≤ λ^{-1} ≤ 880 Å and 71 Å^{-1} ≥ M_L ≥ 57 Å^{-1}.

the scattered intensity standard. The corresponding uncertainty in the radius of gyration is estimated to be around 12%, mostly due to the error in the initial slope determination at infinite dilution.

The mean square radius of gyration in Table I is plotted against molecular weight in double logarithmic scale in Figure 4. The two solid curves are drawn according to eq 6 with λ^{-1} = 880 Å, M_L = 57 daltons/Å, and λ^{-1} = 820 Å, M_L = 71 dalton/Å, respectively. In the same figure, we present the data of Berger and Tidswell[32] in tetrahydrofuran at the same temperature as ours. They are shown in open circles without the uncertainty limits because they do not cite them although we suspect comparable error bounds as in ours. The experimental points are fairly well enveloped by the chosen range of parameters. Subsequent analyses with the particle scattering factor are performed as outlined in the earlier section. Two examples of such curve matchings with the theoretical prediction of Y–F are shown in Figure 5 where the most likely parameters are determined as 790 Å and 78 daltons/Å for λ^{-1}

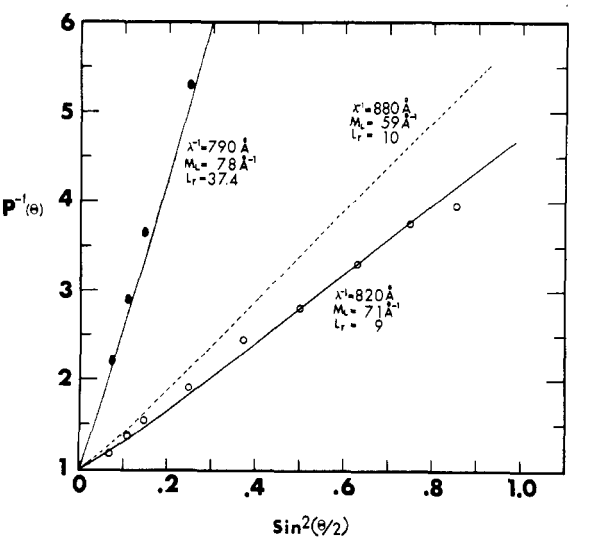

Figure 5. Two examples of the intensity profile matching. The filled circles are for the sample with M_w = 2.3 × 10^6 and the curve is drawn according to the theory of Sharp and Bloomfield, eq 3, with λ^{-1} = 790 Å and M_L = 78 Å^{-1} which correspond to L_r = 37.4 since $L_r = \lambda M/M_L$. The unfilled circles are for the sample with M_w = 5.2 × 10^5, and the solid and chained curves are drawn according to the theory of Yamakawa and Fujii (ref 26), with the parameters as indicated.

and M_L, respectively, for the highest molecular weight samples and 820 Å and 71 daltons/Å for the sample of molecular weight 5.2 × 10^5. The particle scattering factors for the lowest molecular weight samples on the other hand did not produce any sensible matching. A likely explanation may be that the mismatch is due to the optical anisotropy of this sample which was not corrected for but may be quite large at the reduced contour length around 1–3. Unlike small molecular weight fragments of DNA, for which the optical anisotropy is shown to the insignificant,[2] PHIC seems to have sufficient optical anisotropy which must be taken into account at these contour lengths.

Turning to the intrinsic viscosity study, the data in Table I are plotted according to the Y–F scheme in Figure 6. The range of the hydrodynamic diameter 15.6–17.0 Å is chosen; this is based on an earlier result of 10 Å for the same with n-butyl polymer in $CHCl_3$ as determined from the osmotic second virial coefficients of low molecular weight samples. The best ranges of the wormlike-coil parameters which encompass the experimental viscosity and molecular weight data are 790 Å ≤ λ^{-1} ≤ 850 Å and 64 Å^{-1} ≤ M_L ≤ 78 Å^{-1} for the Kuhn statistical length and the mass per unit length, respectively. We plot the data of Berger and Tidswell[32] as obtained in tetrahydrofuran in the same figure.

The effect of variation of the hydrodynamic diameter was examined by lowering the above range by a factor of 2. The result was indiscernible from the one shown in Figure 6; it seems that the diameter cannot be less than 8 Å if the ranges of λ^{-1} and M_L were to be the same as in Figure 6. Given the explicitly represented error limits of the data, we are not able to narrow down the model parameters beyond those cited above. Although it might be difficult to argue for uniqueness of these ranges, clearly a self-consistent set of the model parameters are extracted from the two different experimental methods. Thus we conclude that PHIC in n-hexane and perhaps in THF is characterized by these ranges of the Kuhn statistical length and the mass per unit length, and these results demonstrate the adequacy of the two-parameter description in so far as the equilibrium chain dimension is concerned for the wormlike-coil model.

Turning to the origin of chain stiffness, we note that several models[33–35] have been proposed for the conformational

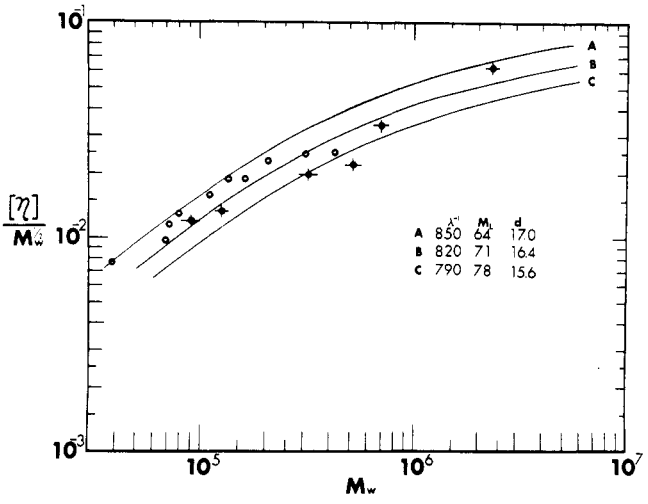

Figure 6. $[\eta]/M_w^{1/2}$ is plotted against M_w where $[\eta]$ is expressed in dl/g units. Three curves with the parameters as indicated are drawn according to the theory of Yamakawa and Fujii (ref 31). Our data are the filled circles and those of Berger and Tidswell (ref 32) in THF are shown as the open circles.

structure based on the energy mapping of a finite segment of the methyl- and ethyl-substituted chains. For the local dimension, these models encompass 1.8–2.3 Å for the monomeric projection whereas our experiments give the range of 1.6–2.0 Å (equivalent to 78 $Å^{-1} \geq M_L \geq 64$ $Å^{-1}$). The experiment is hardly precise enough to settle on any particular model. If one assumes that the chain segment for the conformational energy mapping has been chosen long enough to account for the neighbor correlations, then the linear dimension of a whole chain could be deduced from such mappings. Han and Yu[34] performed a calculation in this spirit based on their model which is the crudest of the three referred to above, since they have considered only the repulsive van der Waals' interactions. Nevertheless, the dependence of the characteristic ratio on chain length follows closely that of the wormlike-coil model, eq 6, and the persistence length is determined to be 410–430 Å from the asymptotic value of characteristic ratio. This is in reasonable agreement with the range that we have determined, 395–425 Å. In comparing the three models, Tonelli[35] however rejects the Han–Yu model on the basis of the very small monomeric dipole moment inferred from the model. This is puzzling because the Han–Yu model is not very different from what Schneider et al.[36] had initially proposed and its monomeric dipole moment is not smaller by two orders of magnitude than the observed one by Yu et al.[37] and Bur and Roberts.[20] Even though the accurate determination of dipole moment may depend on the choice of internal field, Tonelli's criterion is correct in discrediting the Han–Yu model while his calculation of the monomeric dipole moment merits reconsideration. In short, the nonbonded repulsive interactions alone seem to suffice for the characterization of the chain stiffness. If this is indeed the case, then we have on hand the only hitherto known instance of stiff chains without any specific intramolecular interactions such as hydrogen bonding or the base stacking.

There are two other interesting aspects to this macromolecule. The solvent effect[18] on the local dimension is one and the temperature effect[38] is the other. These two aspects will constitute the subject of a future publication.

Acknowledgment. This was in part supported by NSF. One of the authors (D.N.R.) wishes to thank NSF for a predoctoral traineeship. We also thank Miss JoAnn Yamamoto for assistance in obtaining the light scattering measurement of one of the samples.

References and Notes

(1) J. B. Hays, M. E. Magar, and B. H. Zimm, *Biopolymers*, **8**, 531 (1969).
(2) C. W. Schmid, F. P. Rinehard, and J. E. Hearst, *Biopolymers*, **10**, 883 (1971).
(3) H. Benoit, L. Freund, and G. Spach, "Poly(α-amino acids)", G. Fasman, Ed., Marcel Dekker, New York, N.Y., 1967, p 105.
(4) P. Moha, G. Weill, and H. Benoit, *J. Chim. Phys. Phys.-Chim. Biol.*, **61**, 1240 (1964).
(5) M. L. Hunt, S. Newman, H. A. Scheraga, and P. J. Flory, *J. Phys. Chem.*, **60**, 1278 (1956).
(6) A. M. Holtzer, H. Benoit, and P. Doty, *J. Phys. Chem.*, **58**, 624 (1954).
(7) W. Buchard, *Makromol. Chem.*, **67**, 182 (1963).
(8) N. S. Schneider, S. Furusaki, and R. W. Lenz, *J. Polym. Sci.*, **3**, 933 (1965).
(9) L. J. Fetters and H. Yu, *Macromolecules*, **4**, 385 (1971).
(10) P. J. Flory, "Statistical Mechanics of Chain Molecules", Wiley, New York, N.Y., 1969, p 401.
(11) R. L. Jernigan and P. J. Flory, *J. Chem. Phys.*, **50**, 4178 (1969).
(12) R. Y. Lochhead and A. M. North, *Trans. Faraday Soc.*, 1089 (1972).
(13) N. Nemoto, J. L. Schrag, and J. D. Ferry, *Polym. J.*, **7**, 195 (1975).
(14) R. A. Harris and J. E. Hearst, *J. Chem. Phys.*, **44**, 2595 (1966).
(15) J. E. Hearst, R. A. Harris, and E. Beals, *J. Chem. Phys.*, **45**, 3106 (1966).
(16) J. E. Hearst, E. Beals, and R. A. Harris, *J. Chem. Phys.*, **48**, 5371 (1968).
(17) M. V. Volkenstein, "Configurational Statistics of Polymer Chains", Interscience, New York, N.Y., 1963.
(18) It has been proposed that the apparent shortening of local projection length of n-alkyl polymers of isocyanates in chlorinated hydrocarbon solvents might be due to a specific interaction between carbonyl oxygen and chlorine: M. Goodman and S. Chen, *Macromolecules*, **3**, 398 (1970).
(19) To the extent that the persistence length has been shown to be proportional to the ratio of the elastic bending modulus to kT, it depends on temperature: N. Saito, K. Takahashi, and Y. Yunoki, *J. Phys. Soc. Jpn.*, **22**, 219 (1967).
(20) A. J. Bur and D. E. Roberts, *J. Chem. Phys.*, **51**, 406 (1969).
(21) A. J. Bur, *J. Chem. Phys.*, **52**, 3813 (1970).
(22) H. Utiyama, "Light Scattering from Polymer Solutions", M. B. Huglin, Ed., Academic Press, London, 1972, p 78.
(23) D. N. Rubingh, Ph.D. Thesis, University of Wisconsin, 1973.
(24) B. Zimm and D. M. Crothers, *Proc. Natl. Acad. Sci. U.S.A.*, **48**, 905 (1962).
(25) G. C. Berry, *J. Chem. Phys.*, **44**, 4550 (1966).
(26) H. Yamakawa and M. Fujii, *Macromolecules*, **7**, 649 (1974).
(27) P. Sharp and V. A. Bloomfield, *Biopolymers*, **6**, 1201 (1968).
(28) H. E. Daniels, *Proc. R., Soc. Edinburgh, Sect. A*, **63**, 290 (1952).
(29) H. Benoit and P. Doty, *J. Phys. Chem.*, **57**, 958 (1953).
(30) J. A. Harpst, A. I. Krasna, and B. H. Zimm, *Biopolymers*, **6**, 585 (1968).
(31) H. Yamakawa and M. Fujii, *Macromolecules*, **7**, 128 (1974).
(32) M. N. Berger and B. M. Tidswell, *J. Polym. Sci., Polym. Symp.*, **42**, 1063 (1973).
(33) T. C. Troxell and H. A. Scheraga, *Macromolecules*, **14**, 528 (1971).
(34) C. C.-C. Han and H. Yu, *Polym. Prepr., Am. Chem. Soc., Div. Polym. Chem.*, **14**, 121 (1973).
(35) A. E. Tonelli, *Macromolecules*, **7**, 628 (1974).
(36) N. S. Schneider, S. Furusaki, and R. W. Lenz, *J. Polym. Sci., Part A*, **3**, 933 (1965).
(37) H. Yu, A. J. Bur, and L. J. Fetters, *J. Chem. Phys.*, **44**, 2568 (1966).
(38) J. S. Anderson and W. E. Vaughan, *Macromolecules*, **8**, 454 (1975).